JOURNAL OF MATERIALS SCIENCE **39** (2004) 2795–2799

Microstructural studies in low specific energy laser surface treated Al(A356)-SiC_P composites

K. UDAYA BHAT
Department of Metallurgical and Materials Engineering, National Institute of Technology, Karnataka, Suratkal 575 025, India

M. K. SURAPPA
Centre for Advanced Study, Department of Metallurgy, Indian Institute of Science, Bangalore 560 012, India
E-mail: mirle@metalrg.iisc.ernet.in

SiC particulate reinforced A356 Al metal matrix composites were laser treated using pulsed Nd-YAG laser beam. The processing was carried out in air atmosphere at varying pulse energy (5 to 20 J) and scan rates (30 to 150 mm/sec). The samples were cut perpendicular to the track and they were characterized using optical microscopy, scanning electron microscopy and X-ray diffraction. Microstructure of laser treated region consists of regular succession of coarse and fine microstructure signifying the presence of low velocity bands. Transition from cellular/columnar dendritic to equiaxed dendritic structure has been observed. Microstructure of samples laser treated with specific energy greater than 13 kJ/cm^2 show presence of Al_4C_3 platelets.

1. Introduction

Laser surface treatment has emerged as an important and attractive route for materials processing. It provides a unique way of modifying the surface properties of materials. Advantages of laser surface treatments include high hardness, good wear resistance and corrosion resistance properties, fine and novel solidification structures [1, 2]. Laser surface treatment processing has the inherent ability to produce a high solidification velocity (0.01–1 m/s) and a high temperature gradient (up to 10^6 k/m). It is regarded as a situation between welding and splat cooling [1]. It is commonly accepted that a fine cellular/dendritic structure with extended solid solubility will be observed following laser treatments [3]. In the case of particle reinforced metal matrix composites, the presence of ceramic particles will affect the resulting solidification structures. It may alter the movement of the solidifying interface. It may help in the formation of heterogeneous nuclei or partially dissolve and alter the composition of the matrix locally [4]. The purpose of this investigation is to study the formation of various types of solidification structures during low specific energy (4.1 to 33 kJ/cm^2) laser surface treatment of A356Al-SiC_P composites using a pulsed Nd-YAG laser.

2. Experimental procedure

The A356 Al-SiC_P composite material used in this investigation was fabricated by casting route. Cast composite billet was hot extruded into 13 mm diameter rod. Samples for laser treatment were made by cutting the rod into 5 mm thick pieces. Composites contained 10 vol% of 40 micron (average size) SiC particles. The matrix of the composite had approximately 7% Si and 0.7% Mg as the major alloying elements. Laser surface treatment was carried out on the surface perpendicular to the extruded direction. To keep reflectivity constant and uniform the sample surface was polished using 180 grit paper and then ultrasonically cleaned. Line tracks were made using a Nd-YAG laser beam (1.06 μm wavelength), at various scan rates and pulse energies. Scan rates and pulse energies ranged from 30 to 150 mm/min and 5 to 20 J respectively. Laser treatment under various conditions were compared based on specific energy and it is defined as Power/(Scan rate $*$ Beam width) [3] or laser fluence [5]. Specific energy per unit time provides laser intensity. Similarly pulse width and scan rate decide the interaction time between the energy source and the material. The spectrum of conditions (scan rate and pulse energy) produced specific energies in the range from 4.17 to 33.33 kJ/cm^2. The pulse width and pulsing rate were kept constant at 10 milliseconds and 10 Hz respectively. The processing was carried out under open atmospheric conditions. Samples were cut perpendicular to the laser track, metallographically polished and examined using optical and scanning electron microscopy, EDX and XRD. Vickers Micro Hardness values in the laser treated region were measured using a 200 gram load.

3. Results and discussions

The variations in the melt width and melt depth with the pulse energy and scan rates are shown in Figs 1 and 2 respectively. Increase in the pulse energy increases

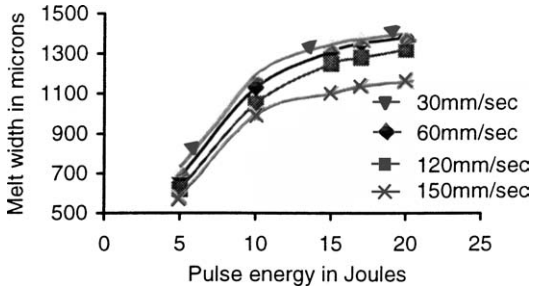

Figure 1 Variation of melt width with pulse energy.

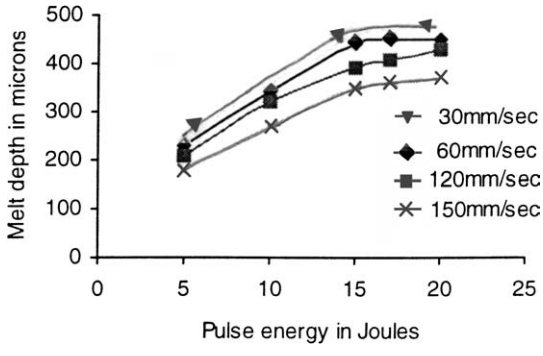

Figure 2 Variation of melt depth with pulse energy.

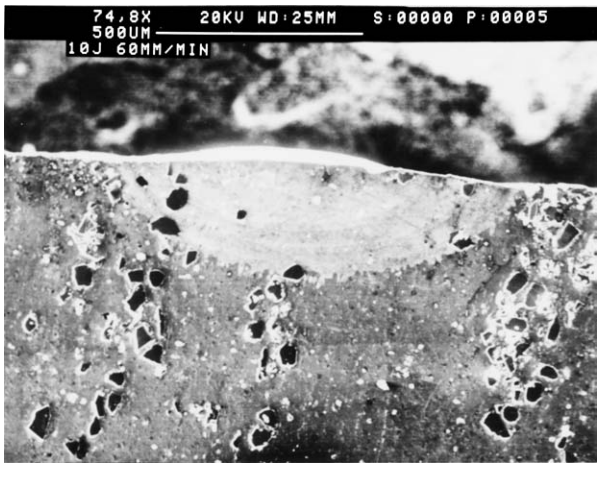

Figure 3 SEM micrograph of a laser treated region.

the melt depth and also surface rippling. An increase in the scan speed results in less interaction time between the laser beam and the material and hence results in the formation of a melt pool of smaller width and smaller depth. It reduces the fluid flow in the material and thus alters the shape of the molten metal pool. Fig. 3 shows an optical micrograph of a typical region after laser melting and re-solidification. The boundary between the re-solidified and the un-melted base material can be clearly seen. Fig. 4 is a micrograph of the laser treated region in a sample treated with a specific energy of 4.17 kJ/cm^2. It shows the formation of alternate regions of fine and coarse microstructures. This is a typical banded structure. The banded structure is characterized by periodicity (either in the scale or in the nature of the structure) along the growth direction. A microstructure consisting of alternate fine and coarse regions is also known as low velocity bands. Oscillations in the local growth rate is responsible for the formation of these low velocity bands [6]. Banded structures have been observed and reported in a variety of alloys including Al-Cu [7], Ag-Cu [8], Al-Fe [9] under rapid solidification conditions. However, until now such banded sequences have not been reported in hypo-eutectic Al-Si alloys. The spacing of one band is defined to be the sum of the lengths of one fine and one coarse band [6]. In the present studies the band spacing is around 35 to 40 μm. The structure is columnar up to a distance of about 100 μm from melt/un-melted interface and thereafter it is completely equiaxed. Even after transition (from columnar to equiaxed), the banded structure (alternate regions of coarse and fine structures) exists in the equiaxed dendritic region.

Microstructure at the interface between melted and unmelted region is cellular (width 1 to 1.5 μm for 4.17 kJ/cm^2) (Fig. 5). There is a transition from cellular to equiaxed dendrites along the direction towards the top surface. This observation can be explained using *G/V* ratio where *G* is the thermal gradient in the liquid near the growing interface, and *V* is the velocity of the solidifying interface [10]. At low specific energy, the amount of superheat in the melt is less. Low superheat coupled with the high conductivity of the material (which leads to more uniform temperature), reduces the thermal gradient in the liquid near the melt/unmelted interface. Additionally, initial convection in the melt pool will eliminate whatever thermal gradient present in the melt. Because of the epitaxial nucleation and growth, the interface velocity increases rapidly. This leads in low *G/V* ratio at the beginning of the solidification and results in cellular structure. After some amount of solidification, the heat from the remaining liquid will be rapidly taken away by the surrounding high conducting material giving a high *V* value and the structure changes from cellular to equiaxed dendritic. The transition from the cells to dendrites have been modelled and it occurs when the interface velocity increases as growth increases [10].

The structure at the center of the re-solidified region is equiaxed dendritic (Fig. 6). Explanation based on *G/V* value is already given in the earlier paragraph. Further there is some possibility of nonmetallic particles like oxides present in the melt acting as heterogeneous nucleation sites. During their growth, the interface growth direction and bulk heat transfer directions become parallel to each other [11]. This gives rise to equiaxed dendritic structure at the center of the track. Another possible reason for the formation of equiaxed dendritic structure is the thermo-elastic strains in the material due to successive laser pulses. The laser pulse falling on the material suddenly increases the temperature of small region of the material and causes melting. This produces a small amount of thermo-elastic strains to produce ultrasonic waves [12]. This ultrasonic waves pass through the material and they break the dendrite tips. These tips will be moved on to the center and they acts as nuclei. They give rise to randomly oriented dendrites. Possibility of the fragmentation of the growing crystals and these additional features acting as the nucleating site for equiaxed crystals has been reported earlier [11].

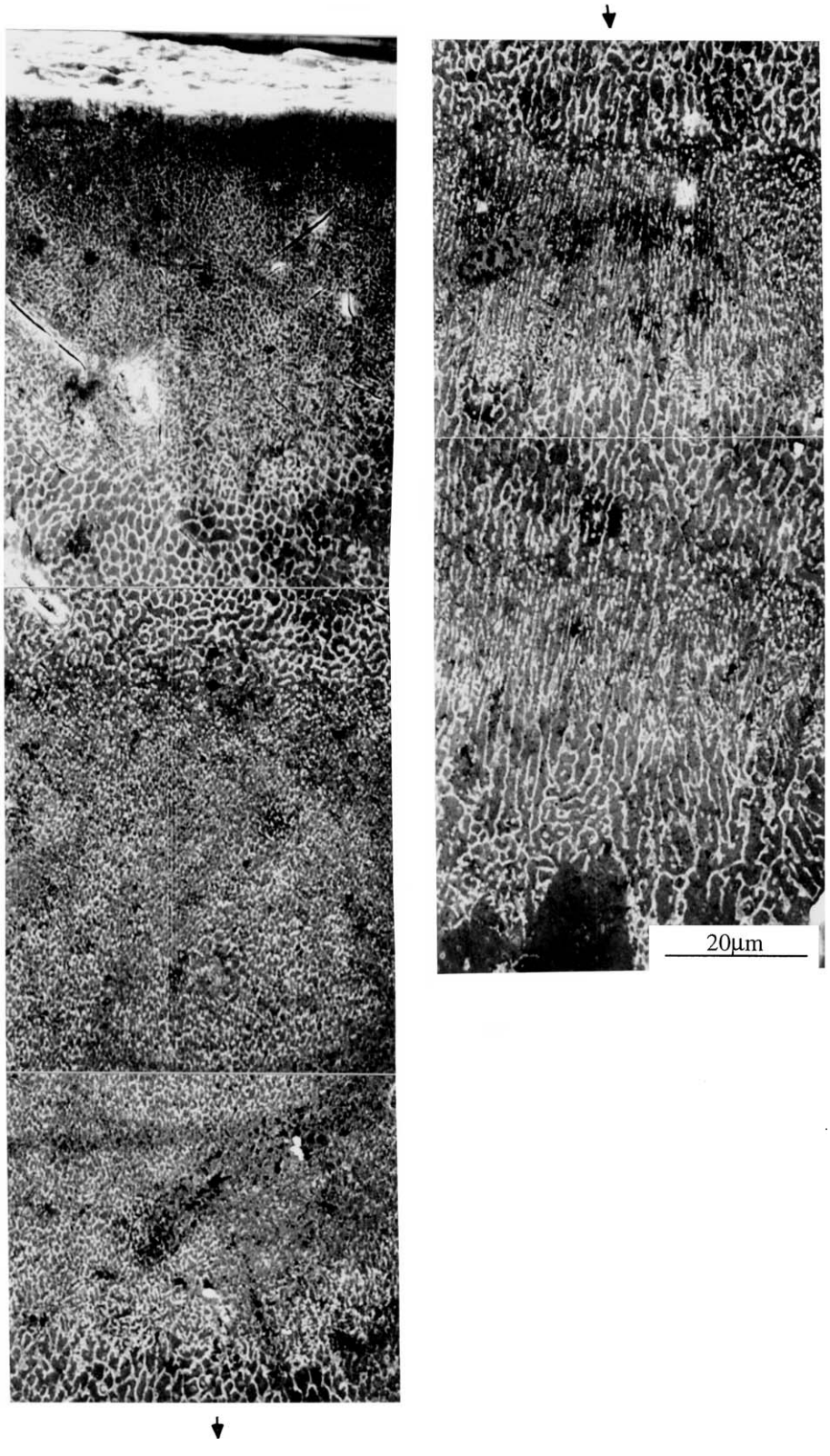

Figure 4 Micrograph showing banded microstructure.

In all samples gas pores are seen (Fig. 6). This could be due to hydrogen entrapment since processing was done under open atmospheric conditions. During solidification of the re-melted region the silicon comes out in the form of plates in the inter-dendritic or intercelluar region.

Microstructure shows needle like particles up to a distance of 100 μm from the top surface. These needle like particles were identified to be aluminium carbide. Size and density of aluminium carbide needles vary with distance from the top surface. In general needles were thicker and shorter at the top surface. Thinner and longer needles wee observed at a distance slightly away from the top surface and along the depth direction.

During laser treatment, the reinforced SiC particles were partially dissolved and aluminium carbide needles (Fig. 7) were formed according to the following

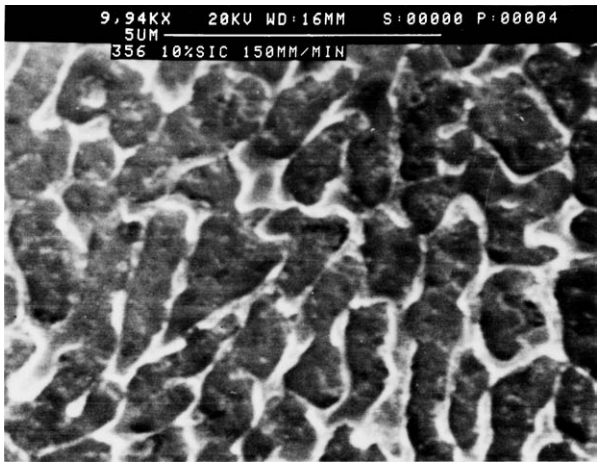

Figure 5 Micrograph showing cellular structure at the treated/untreated interface.

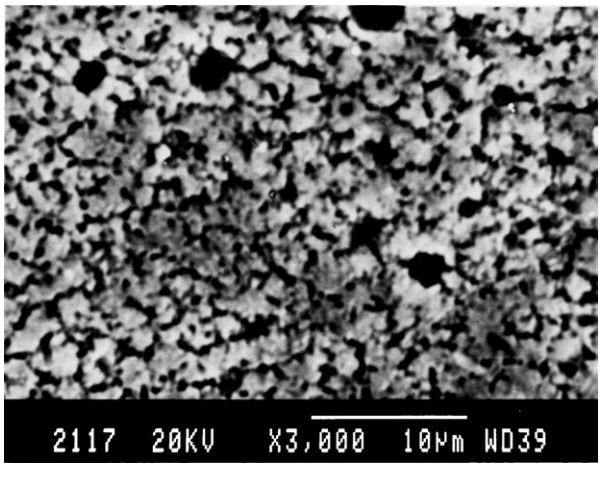

Figure 6 Micrograph showing equiaxed dendrites and pores at the center of the treated region.

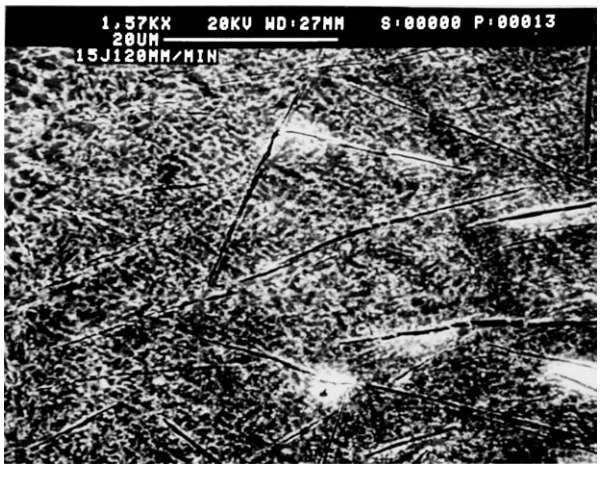

Figure 7 Micrograph showing the Al_4C_3 in the treated region.

reaction [13–15]

$$3SiC + 4Al \rightarrow Al_4C_3 + 3Si$$

The formation of carbides is reported by many authors during high specific energy treatment [1, 16, 17]. The dissolution of SiC is increases with the increase in the specific energy and results in the formation of Al_4C_3 needles of larger size (approximately 40 μm length at 33.33 kJ/cm^2 and 5 μm length at 16 kJ/cm^2 respectively) and more in number (Fig. 7). This is because at high specific energy conditions, due to larger amount of heat, dissolution of SiC is more and it increases activity of the carbon in the melt and also it increases the time required for re-solidification. This favours the nucleation and growth of aluminium carbide particles. The Al_4C_3 particles are straight and show a random orientation within the re-solidified region. Formation of Al_4C_3 of random orientation is also reported by Ocelik *et al.* [18], in SiC/Al metal matrix composite produced by laser melt injection. Concomitantly when SiC gets dissolved, melt gets enriched with Si and it is confirmed by EDX analysis. A high heat input destroys SiC particulates completely and forms large (both in size and quantity) amounts of Al_4C_3 platelets in the fusion zone. The larger size and high volume fraction of Al_4C_3 are deleterious to the MMC because they degrade the engineering properties of the material. With decreased specific energy, the size and amount of Al_4C_3 decreases and it exists along with physically altered (partially dissolved) SiC particles in the Al alloy matrix.

In the present studies, specimens treated with specific energy less than 13 kJ/cm^2 SiC particles are partially dissolved but the extent is very low to produce aluminium carbides. The high silicon content in the base alloy reduces the tendency for carbide formation [14]. Partial dissolution of SiC was confirmed by the increased concentration of Si in the re-solidified region (approx. 0.5% in the case of 4.17% kJ/cm^2 specific energy treatment). This is again observed in EDX analysis. By controlling the laser specific energy it is possible to control the dissolution of SiC particles and there by the size and amount of the Al_4C_3 particles in the fusion zone. It is reported [16] that optimum level of properties will be attained by having both SiC and Al_4C_3 acting as reinforcement phases in a microstructurally modified matrix material. Role of Al_4C_3 phase as a reinforcement has been discussed by Bestera *et al.* [19].

4. Hardness measurements

Vickers Micro-Hardness measurements were done in the melted and re-solidified region. There is considerable increase in the hardness due to laser treatment and this can be explained as follows. Firstly a refinement in structure occurs, causing an increase in hardness. Secondly the presence of aluminium carbide particles up to a certain distance from the top surface contributes to increase in hardness. In the region free from aluminium carbide particles enhanced hardness comes due to the refinement of microstructure.

5. Conclusions

1. Low velocity bands consisting of regular succession of coarse and fine structures has been observed.

2. At the melt/un-melted interface the structure was cellular/columnar dendritic. Transition from cellular/columnar dendrite to equiaxed dendrite takes place

at some distance (depending on specific energy) from the melt/un-melted interface.

3. Samples treated with energy more than 13 kJ/cm^2 show the presence of Al_4C_3 particles.

References

1. H. J. HEGGE and J. TH. M. DE HOSSOM, *Scripta Met. et Mater.* **24** (1990) 593.
2. E. M. R. SILVA, W. A. MONTERIO, W. ROSSI and M. S. F. LIMA, *J. Mater. Sci. Lett.* **19** (2000) 2095.
3. P. A. MOLIAN, *ibid.* **4** (1985) 265.
4. K. MOHAMMED JASIM, R. D. RAWLINGS, R. SWEENY and D. R. F. WEST, *ibid.* **11** (1992) 414.
5. A. H. WANG and T. M. YUE, *ibid.* **20** (2001) 1965.
6. M. GRMAUD, M. CARRARD and W. KURZ, *Acta Metall. Mater.* **38** (1990).
7. M. CARRARD, M. GREMAUD, M. ZIMMERMANN and W. KURZ, *ibid.* **40** (1992) 983.
8. D. G. BECK, S. M. COPLEY and M. BASS, *Metall. Trans.* A **13** (1982) 1879.
9. M. GREMAUD, M. CARRARD and W. KURZ, *Acta Metall. Mater.* **38** (1990) 2587.
10. W. KURZ and R. TRIVEDI, *Mater. Sci. Engng.* A **179** (1994) 46.
11. W. C. WINE GUARD, "An Introduction to the Solidification of Metals," The Institute of Metals (1964) p. 64.
12. H. KOEBNER, "Industrial Applications of Lasers" (John Willey & Sons, 1984) p. 154.
13. J. S. AHEARN, C. COOKE and S. G. FISHMAN, *Metal Constr.* **14** (1982) 192.
14. T. ISEKI, T. KAMADA and T. MARUYAMA, *J. Mater. Sci.* **19** (1984) 1692.
15. LI HONG, R. M. VILLAR and WANG YOUMING, *ibid.* (1997) 1965.
16. NARENDRA B. DAHOTRE, T. DWAYNE MCCAY and MARY HELEN MCCAY, *J. Appl. Phys.* **65** (1989) 5072.
17. T. J. LIENERT, E. D. BRANDON and J. C. LIPPOLD, *Script. Met. et Mater.* **28** (1993) 1341.
18. V. OCELIK, J. A. VREELING and J. TH. M. DE HOSSON, *J. Mater. Sci.* **36** (2001) 4845.
19. M. BESTERCI and J. IVAN, *J. Mater. Sci. Lett.* **15** (1996) 2071.

Received 5 March 2003
and accepted 5 January 2004